JOURNAL OF MATERIALS SCIENCE: MATERIALS IN MEDICINE 3 (1992) 255–261

Continuous and discontinuous fatigue crack growth of irradiated ultrahigh molecular mass polyethylene in saline solution at 37 °C

Z. P. ZENG, M. BUGGY, J. GRIFFIN, E. G. LITTLE
Department of Mechanical and Production Engineering, University of Limerick, Limerick, Republic of Ireland

To provide data for prosthesis design, the fatigue crack growth resistance of irradiated ultrahigh molecular mass polyethylene (UHMMPE) in saline solution at 37 °C was determined from tests performed on compact tension specimens, comparable in size to the components in knee prostheses. The specimens were cyclically loaded by using a sinusoidal wave form at 1 Hz with a minimum-to-maximum load ratio of 0.1. Scanning electron microscopic fractography was used to examine the fracture surfaces. At higher stress levels, the Paris's Law was used to analyse the data, and a striation pattern with each striation corresponding to multi-cycles was observed. At lower stress levels, discontinuous fatigue crack growth was found, a phenomenon which dominated the fatigue life of the material and had not been reported previously in this material. A craze zone ahead of the crack tip was observed, which formed the discontinuous crack growth band with a length relevant to the Dugdale plastic zone length.

1. Introduction

Ultrahigh molecular mass polyethylene (UHMMPE) is widely used for making load-bearing components such as in human joint prostheses [1], where the components are subjected to periodical loading. Examination of UHMMPE components from joint replacements has revealed several modes of damage [2–5] including degradative fatigue.

Fatigue crack growth (FCG) testing of UHMMPE has been performed in air [6]. However, as the FCG behaviour of polymers is a function of material variables, in this work the FCG testing of UHMMPE was carried out in conditions more relevant to the body environment and under a broader loading conditions than in the previous studies.

Crack growth resistance is determined by continuously monitoring the growth of a crack from a notch (pre-cracked) as the specimen is cyclically loaded. In linear elastic fracture mechanics, the curve of FCG rate (da/dN) versus applied stress intensity factor (K) range with three distinct regions has been used to illustrate the FCG property [7]. The region at low ΔK represents the threshold for FCG, ΔK_{th}; and the region at high ΔK, as the applied maximum K approaches the fracture toughness, K_{1c}, of the material, is characterized by very rapid FCG rates. The middle region, which is of major concern in FCG research, is characterized by the important relationship shown by Paris [8, 9], which relates FCG rates to the prevailing stress intensity factor conditions at the tip of a growing crack as in Equation 1:

$$da/dN = C \times \Delta K^m \quad (1)$$

where C and m are material constants. FCG is continuous in this loading region with a striation mechanism [10] in which each striation length for a loading cycle is equal to the present macroscopic FCG length during that loading cycle. Paris's Law has been used in the study of FCG in several engineering plastics [11], although these materials are clearly not linearly elastic. At relatively high ΔK levels, in many polymers, FCG is continuous and reveals fatigue striation spacings that are in excellent agreement with microscopically determined crack growth rates [17]. However, when the driving force is reduced below a critical threshold value, crack advance cannot occur on each cycle and the crack arrests [12]. At low ΔK levels in several polymeric solids [13], a second set of fracture bands has been observed which did not correspond to the prevailing macroscopic growth rate in that ΔK regime, but reflected discrete increments in crack advance that appeared after several hundred to several thousand cycles of total crack arrest. This cumulative damage mechanism was reported to enable crack advance after a multiple number of loading cycles even if the driving force is unable to propagate the crack on each cycle [12]. Such a FCG process is called discontinuous crack growth (DCG) which results in a distinct fractured surface structure, the DCG bands [13, 14], of which the width has been reported to

0957–4530

correspond to the Dugdale plastic zone length [16] as given in Equation 2:

$$\text{Plastic zone length} = \pi \times K^2/(8 \times \sigma_y^2) \quad (2)$$

where K in this case is the present maximum stress intensity factor during cyclic loading and σ_y is the yield strength of the material. Subsequent studies [17] revealed that these bands were produced by continuous growth of a craze zone ahead of the advancing crack front, followed by sudden breakdown of the craze. DCG bands were developed in polycarbonate and polysulfone which formed in association with a pair of shear bands above and below the crack plane and the combination of the two shear bands and associated craze band were referred to as a ε-discontinuous growth band [18, 19].

2. Experimental details

Specimens of UHMMPE were machined from a compression-moulded block and were processed and irradiated in the same way as the prosthesis component and were irradiated [20]. Tensile tests on the material in air at 37 °C were carried out [21] and the yield strength σ_y was calculated to be 22.04 MPa.

The FCG experiments [22] were carried out by using a sinusoidal wave form, with cyclic loading at 1 Hz and a minimum-to-maximum load ratio of 0.1. Experiments were performed on compact tension specimens (40 mm × 40 mm × 10 mm thickness with a crack length of 7 mm) comparable in size to the components in knee prostheses. Each specimen was pre-cracked with a new sharp razor blade. Although basically similar, there were a few major experimental differences between the present experiments and previous ones of other researchers [6]; in this study the material was irradiated and the testing was performed in saline solution at 37 °C with a loading frequency of 1 Hz.

Measurements of crack length were made with a ×32 travelling microscope. A computer program, using the seven incremental point polynomial method [22], was used for analysing the data of crack length versus the loading cycles. To determine the mechanisms of FCG, during the fatigue loading process the shape of the crack tip region (profile views) were photographed at frequent intervals through the travelling microscope. The experimental set-up can be seen from Fig. 1. After testing, the fracture surfaces, sputter coated with gold, were examined in a scanning electron microscope.

3. Results

At the higher loading levels, when the amplitudes of the applied load (P_a) were not less than 400 N, a relationship between da/dN and ΔK at the crack tip was calculated from the data of crack length (a) versus loading cycles (N) as shown in Fig. 2. A typical fractograph of these specimens is shown in Fig. 3 and displays pronounced lines perpendicular to the FCG direction which can be seen all over the fracture surface. At the lower loading levels, when $P_a \leq 350$ N, the FCG during the first part of the experiment was

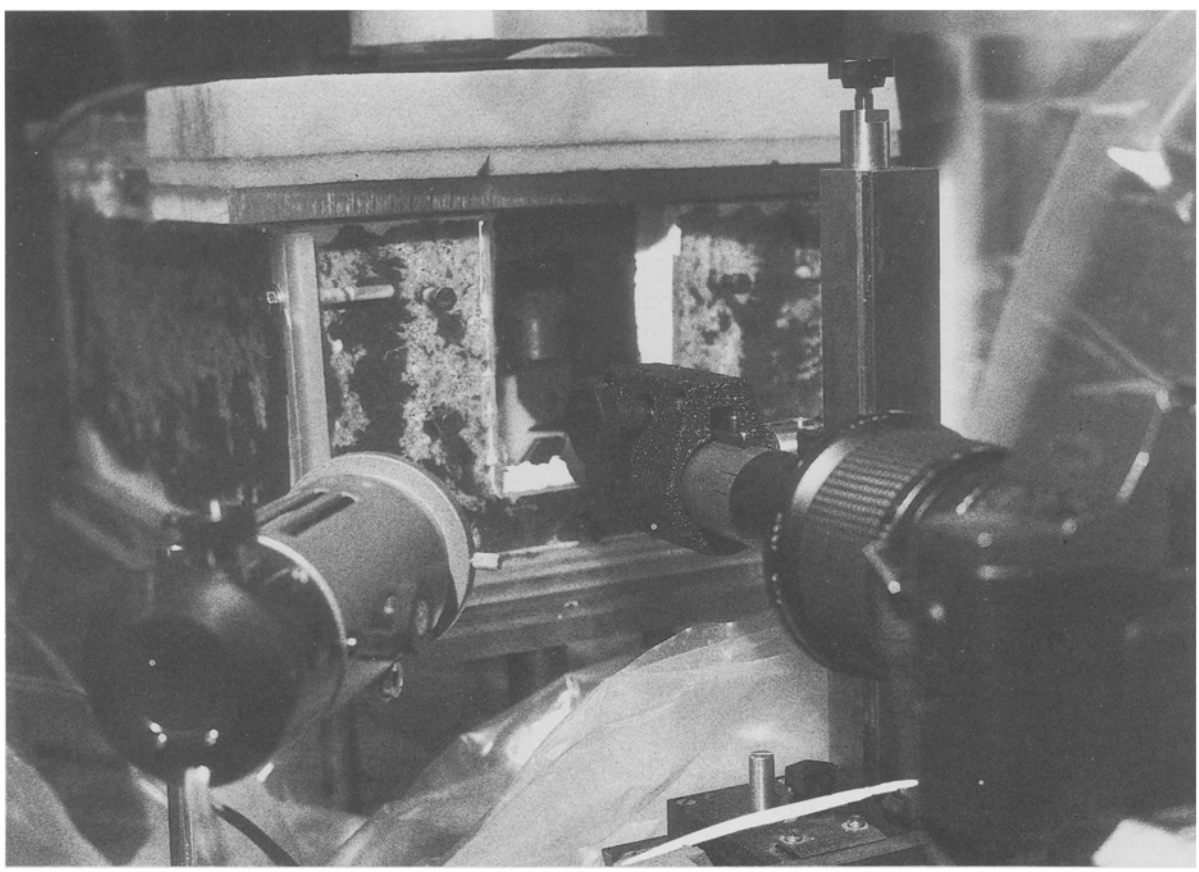

Figure 1 Experimental set-up including the Mand testing machine, environmental chamber, travelling microscope and camera.

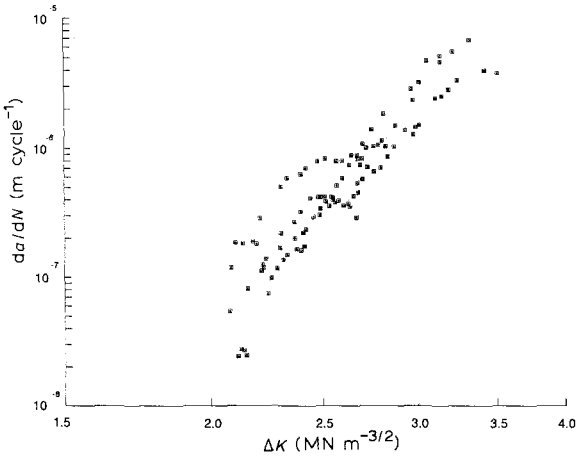

Figure 2 FCG rate versus ΔK for experiments at higher ΔK levels.

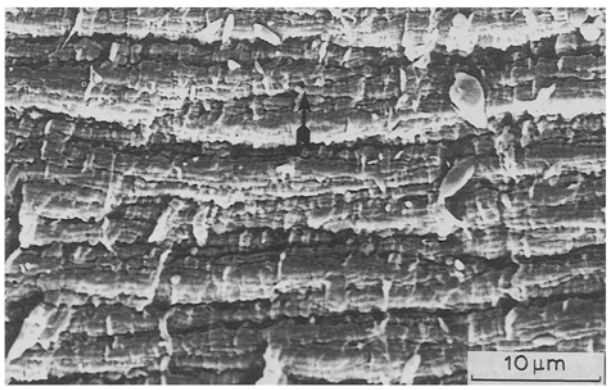

Figure 3 Scanning electron microscopic fractography showed that at the higher loading level a striation pattern with one striation related to multi-cycles. (Arrow indicates the crack growth direction.)

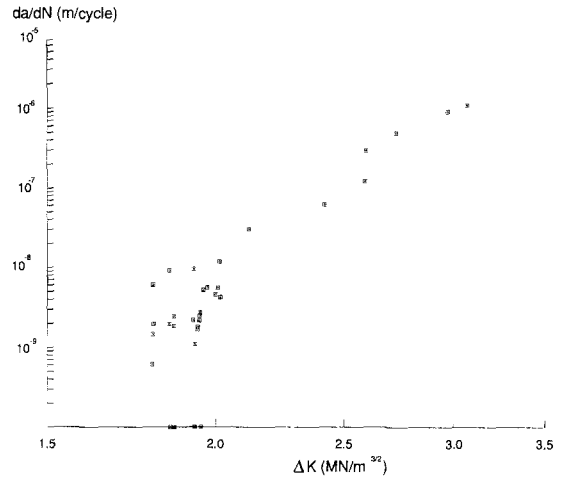

Figure 4 FCG rate versus ΔK for an experiment at a lower ΔK level.

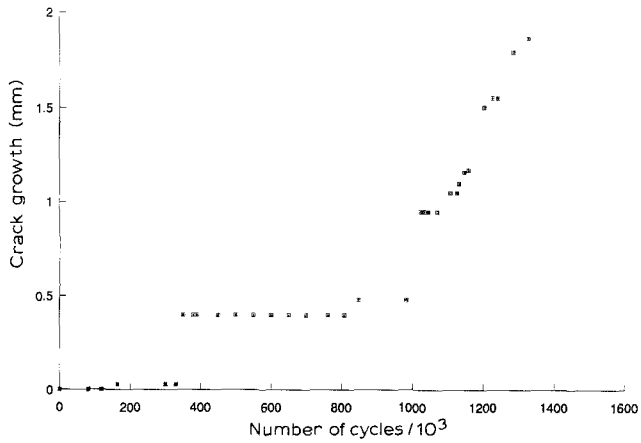

Figure 5 Fatigue crack length versus the passed loading cycles for an experiment at a lower ΔK level.

observed to be discontinuous, which had not been reported in previous studies on this material [6]. The seven incremental point polynomial method was used to analyse data of crack length versus ΔK even in the DCG range. As the program uses average results both for da/dN and ΔK, it was rewritten to let the extremely low FCG rates, which are less than 1×10^{-9} m cycle^{-1}, to be zero, thus revealing the nature of DCG. Frequent observations of the crack length were used so that the contrast between crack arresting and crack jumping did not become ambiguous as a result of the data averaging. In Fig. 4, the graph of crack growth rate versus ΔK shows that initially, where the ΔK was at the lowest level, the crack growth rate varied between 0 and 1×10^{-8} m cycle^{-1} regardless of the present ΔK value and indicates that during the process of FCG, the crack was arrested between two periods of crack growth. Finally the microscopically continuous growth period can be seen at the higher ΔK level as the crack length increases.

The phenomenon of DCG is further illustrated in Fig. 5, which shows the curve of crack length versus loading cycles. In the early part of the lifetime, the horizontal lines indicate the crack arrest, and the links between these lines show the evidence of the breakthrough of the arrested crack.

The profile views (Fig. 6) of the specimen show the different stages of FCG: the pre-crack had been blunted into a typical square-shaped crack front and arrested until a sharp crack was created from the blunted front as in Fig. 6a. The sharp crack was initially blunted into a typical square-shaped crack front as in Fig. 6b, when an obviously damaged area appeared at the crack tip, until at last a new crack was created at the area of damage as illustrated in Fig. 6c. The process, which can occur several times, appears to take up the majority of the fatigue life, which is much longer than what was expected from the results obtained from the continuous propagation regime. Another series of profile views of a specimen (Fig. 7) also show the DCG process, the region in the vicinity of and ahead of the crack tip was obviously damaged and was also linked together in Fig. 7c. DCG was observed in all tests carried out in saline solution at the low loading level. Damaged zones in the specimen were regarded as the craze zones, and fibrils were considered to exist in the damaged zone. The fibrils were not easy to detect visually in the whole zone as the specimens were relatively thick. However, fibrils were very clear at the area near to the crack tip shown in Fig. 8.

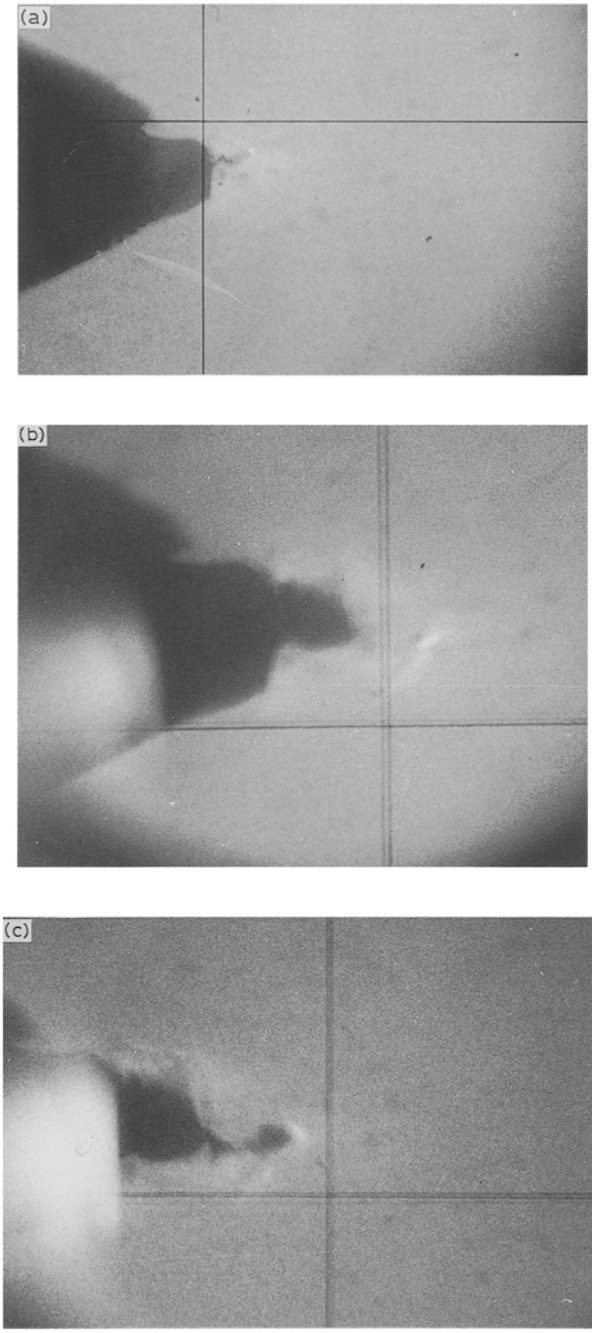

Figure 6 Blunting and re-initiating phenomenon of FCG test of a specimen (the procedure repeated and the total phenomenon lasted 95% of total FCG life of 1 728 000 cycles, total FCG length was 10 mm). (a) First re-initiating at 10% of FCG life and 3.7% of total FCG length. (b) Crack blunted, new crack initiating at 63.3% of FCG life and 4.5% of total FCG length. (c) New crack initiated at 79.1% of FCG life and 9.2% of total FCG length.

Fractography showed distinct differences between the two regions, the one with macroscopically continuous crack growth and the other one with DCG as in Fig. 9. In the continuous FCG area, there was a striation pattern with each single striation corresponding to several loading cycles. Little deformation can be seen on these fractured surfaces, implying that the fracture at these higher stress levels was essentially brittle; while in the DCG region, extensive plastic deformation by extension of fibrils and cavitation can be seen.

Pronounced bright lines on the specimens at both sides of the crack tip at 45° to the crack growing plane were observed before the crack started to initiate from the notch at the loading levels of $P_a \geqslant 350$ N, but did not occur at the loading levels where $P_a \leqslant 300$ N. These 45° lines can be explained as the influence of the shear stress at the crack tips.

4. Discussion

When ΔK is greater 2 MN m$^{-3/2}$ and P_a was not less than 400 N, the FCG behaviour in UHMMPE in saline solution at 37 °C, seen as in Fig. 2, was similar to that has been reported by previous researchers [6] for the tests of the un-irradiated UHMMPE. The crack growth rate was macroscopically continuous and increased as ΔK increased; the slope m in Equation 1 was determined to be 9.7, and setting $da/dN = 10^{-9}$ m cycle^{-1} to the threshold, ΔK_{th} was calculated to be 1.36 MN m$^{-3/2}$. The fractographic observations (Fig. 3) showed pronounced lines on the fractured surfaces with each line corresponding to multi-cycles [6], the line spacings are statistically constant in the whole fractured surface and an average length of 3 μm was measured. It has also been reported elsewhere for the un-irradiated UHMMPE tested in air that spacings of these lines were at least 10 times bigger than the present FCG length per cycle and were irrelevant to the apparent ΔK level [6]. These lines were therefore unrelated to the FCG rate which is dependent on the value of ΔK during continuous crack FCG. As described in Equation 2 for DCG, the DCG band length has been reported to be related to the Dugdale plastic zone length [16]. Taking the maximum peak value of K as 2.2 MN m$^{-3/2}$, which is less than the minimum recorded peak value of K at these higher stress levels, the minimum Dugdale plastic zone length was calculated to be 3 mm which is about 1000 times bigger than the line spacings on the fractured surfaces, indicating that the line pattern on the fracture surface at these loading levels was by no means related to the Dugdale plastic zone. Therefore the lines can not be regarded as DCG bands [15, 11] and the crack growth was not DCG for these loading conditions. When $\Delta K < 1.9$ MN m$^{-3/2}$ and $P_a < 350$ N the DCG was observed and the original crack was blunted and arrested until a new sharp crack was created from the blunted crack front as in Fig. 6. This kind of DCG was observed in all the experiments in the saline solution at the lower load levels of this study.

Craze formation, of which the existence in the non-glassy polymers such as high density polyethylene and UHMMPE can hardly be doubted [23], has been regarded as the basis of DCG [17]. The stress-whitened regions which have been reported as strong evidence of crazes [23] were observed in this study. For crystalline polymers similar to UHMMPE, work has also shown evidence of crazing in environmental stress cracking in both low and high density polyethylene [24] and crazing has been demonstrated in the fracture of polyethylene in the absence of environmental

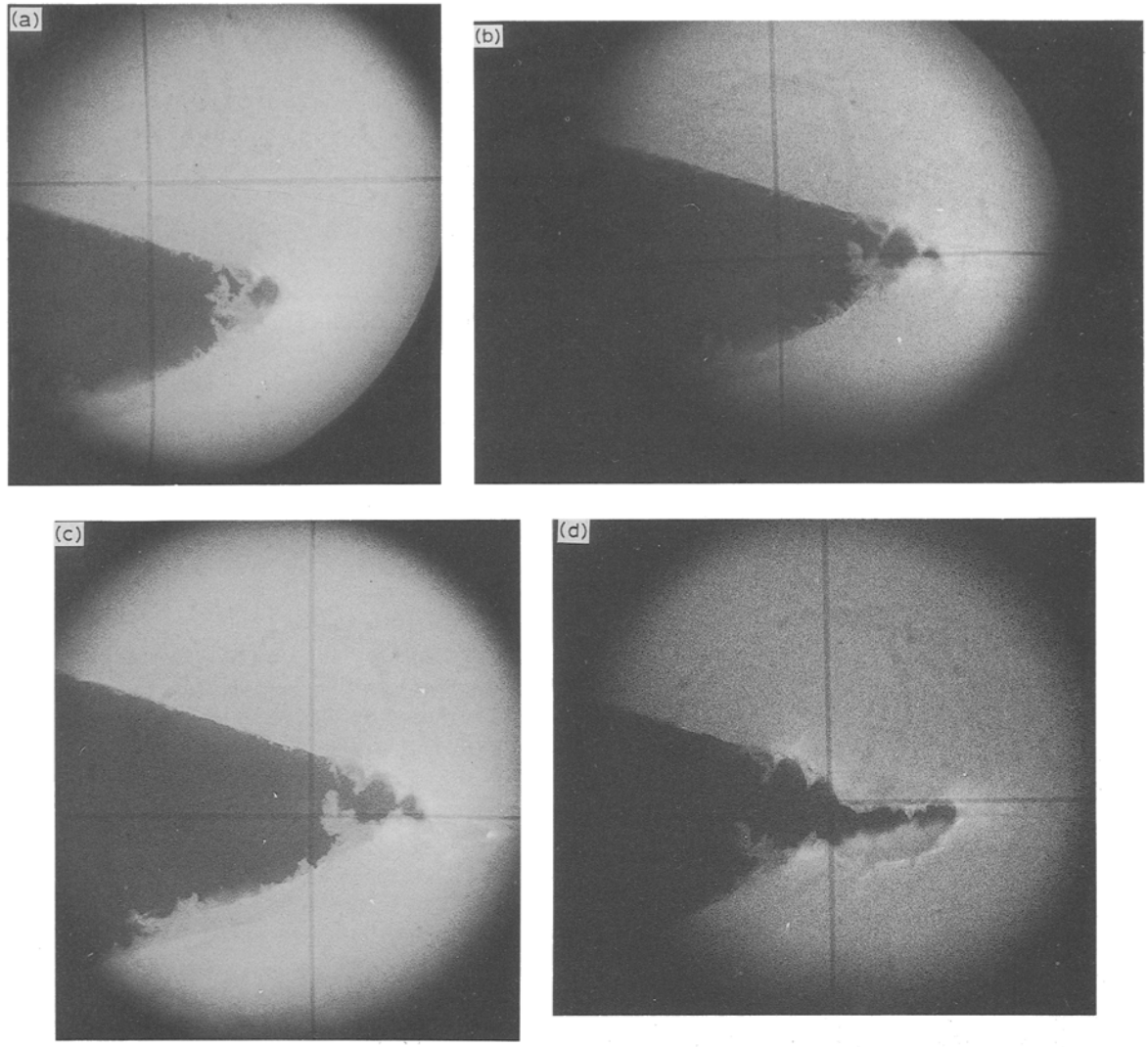

Figure 7 Profile views of a specimen showing the formation and breakthrough of a damaged region at the crack tip: (a) crack before initiation; (b) crack after initiation; (c) damaged zone before the crack tip; (d) the breakthrough of the damaged zone.

Figure 8 A profile view of a specimen shown fibrils at the damaged region near the crack tip.

Figure 9 Scanning electron microscopic fractography showed distinct fracture surfaces at the region of continuous FCG and that of DCG. (Arrow indicates the crack growth direction.)

stress cracking agents [25]. Profile views of the specimens during the fatigue process, as in Fig. 7, show that the regions immediately ahead of the crack tips were obviously damaged but were also linked together by the remaining material, supposedly fibrils. The formation of the damaged zone is similar to the sketches of craze formation reported by other authors [11] and the craze structure of medium density polyethylene during stress cracking under constant tensile loading in air [26]. The fibrils observed in these damaged zones (see Fig. 8), mostly at the crack tip, were also similar to reported observations in the medium dens-

ity polyethylene and were further evidence of craze. So crazes undoubtedly exist in this crystalline polymer [26] and craze bands formed under the fatigue loading in this study as shown in Fig. 5.

From Fig. 5 the lengths of crack advance during crack jumping between the two crack arrest periods were both around 0.5 mm. As the lower stress levels, the Dugdale plastic zone length at the beginning of FCG should be less than 3 mm, the length as calculated for the higher stress levels. It can therefore be seen that the crack jumping distances were related to the Dugdale plastic zone length and therefore similar to the DCG observed by researchers in other materials [15, 11].

At these lower loading levels, while DCG was observed at the first part of the lifetime, continuous FCG was also observed at the second part where the ΔK increased as the crack length increased, as in Fig. 5. The fractograph (Fig. 9) showed distinctly different features between the first region of macro-arresting and the second region (with striations), and provided further evidence that the crack growth mechanisms in the regions are different.

It has been reported that the crack growth in medium density polyethylene was discontinuous during stress cracking by a mechanism of continuous growth of craze zones ahead of the arrested crack tip before the final breakdown of the craze zones [26]. The same mechanism has been reported in DCG of fatigue tests in plastics [17]. The craze thickness was supposed to increase cyclically until it reaches its ultimate value. The key to the sudden breakdown of the band was believed to correspond to a cyclic strain-induced stretching of the craze fibrils to their ultimate length, t_{max}, which was less than the maximum crack opening distance, D_{max}, for the given ΔK level. A condition of $t_{max} > D_{max}$ has been reported to exist under low test loading frequency conditions when the material possessed either a high molecular mass or high molecular mass tail in a lower average molecular mass polymer [14, 27, 11]. Continuous crack growth should occur and no DCG bands would be expected under a condition where $t_{max} > D_{max}$. However, as DCG was observed in this investigation, the condition of $t_{max} > D_{max}$ could not have occurred in irradiated UHMMPE during these loading conditions, although UHMMPE is a high molecular mass polymer, and the loading frequency of 1 Hz, was also relatively low. Therefore the condition where $t_{max} < D_{max}$ and DCG can also exist under relatively low loading frequency conditions and when the material possesses high molecular mass, although it has not been reported in testing of un-irradiated UHMMPE in air by previous researchers using a higher loading frequency, 5 Hz [6].

Distinct lines at 45° with respect to the cracking plane were noticed and provided strong evidence of the existence of shear [28]. When P_a was 350 N, the ε-discontinuous growth bands were formed by the craze band and the two shear bands as the crack arrested and the shear process was activated from the crack tip and beside the craze. The shear stress blunted the crack front so that the actual ΔK was much less than the nominal ΔK and the crack could arrest up to about 10^6 cycles. The crack tips were blunted because of the existence of the DCG bands, as seen in Figs 6 and 8, where the shape of the tips were square. Adequate stress, temperature and other conditions are the basis of shear blunting during the craze and shear competition [29]. As to the stress level influence, exceedingly low ΔK is essential for the formation of craze. On the other hand, when craze exists, higher stress leads to shear affect. Shear stress effects were observed to appear under at the higher stress levels ($P_a \geqslant 300$ N). At the higher stress levels, the craze bands were not clearly observed, although shear influence was detected during the crack initiating period, clear ε-discontinuous growth bands could not be observed. When the loading levels were very low ($P_a = 300$ N), craze bands were very clear; however, shear bands could not be observed and no ε-discontinuous growth bands were noticed.

5. Conclusions

1. Paris's Law fits the results of fatigue crack growth of irradiated UHMMPE at higher stress levels with a striation pattern in which each striation corresponds to multi-cycles.
2. At lower stress levels the fatigue crack growth of irradiated UHMMPE at 37 °C in saline solution is discontinuous.
3. Crazing plays a considerable role in the fatigue behaviour of UHMMPE.
4. At the medium stress levels, when craze-induced discontinuous crack growth exists, shear at both sides of the crack tip with 45° angles to the fracture plane can at certain times blunt the crack tip, decrease the actual stress at the tip, and arrest the crack growth for up to 10^6 cycles.
5. Distinctly different fractographs were obtained from the region of discontinuous crack growth and the region of continuous crack growth.

Acknowledgement

The authors thank Howmedica Int. Inc., Limerick, for supporting this work.

References

1. S. A. V. SWANSON and M. A. R. FREEMAN, in "The scientific basis of joint replacement" (Pitman Medical Publishing Co. Ltd, Kent, UK, 1977) p. 15.
2. P. DUCHEYNE, A. KAGAN and J. A. LACY, *J. Bone Joint Surg.* **60** (1978) 384.
3. R. M. ROSE, A. CRUGNOLA, M. RIES, W. R. CIMINO, I. PAUL and E. L. RADIN, *Clin. Orthop.* **145** (1979) 277.
4. E. A. SALVATI, T. M. WRIGHT, A. H. BURSTEIN and B. JACOBS, *J. Bone Joint Surg.* **61** (1979) 1239.
5. B. WEIGHTMAN, D. P. ISHERWOOD and S. A. V. SWANSON, *J. Biomed. Mater. Res.* **13** (1979) 673.
6. G. M. CONNELLY, C. M. RIMNAC, T. M. WRIGHT, R. W. HERTZBERG and J. A. MANSON, *J. Orthop. Res.* **2** (1984) 119.
7. R. C. RICE, in "Fatigue design handbook", 2nd edition (Society of Automotive Engineers, Inc., Warrendale, Pennsylvania, USA, 1988) p. 22.
8. P. C. PARIS, in Proceedings of the 10th Sagamore Army Materials Research Conference, New York, 1964 (Syracuse University Press) p. 107.

9. P. C. PARIS and F. ERDOGAN, *J. Basic Engng Trans. ASME* D **85** (1963) 528.
10. C. LAIRD and G. C. SMITH, *Phil. Mag.* **7** (1962) 847.
11. R. W. HERTZBERG, in Proceedings of the 6th International Conference on Fracture, 4–10 December 1984, New Delhi, India, p. 163.
12. M. T. TAKEMORI, *Polym. Engng Sci.* **27** (1987) 46.
13. R. W. HERTZBERG and J. A. MANSON, in "Fatigue of engineering plastics" (Academic Press, New York, 1980) p. 160.
14. M. D. SKIBO, R. W. HERTZBERG, J. A. MANSON and S. KIM, *J. Mater. Sci.* **12** (1977) 531.
15. J. P. ELINCK, J. C. BAUWENS and G. HÒMES, *Int. J. Frac. Mech.* **7** (1971) 277.
16. D. S. DUGDALE, *J. Mech. Phys. Solids* **8** (1960) 100.
17. R. W. HERTZBERG, M. D. SKIBO and J. A. MANSON, *Amer. Soc. Testing Mater. STP* **675** (1979) 471.
18. D. S. MATSUMOTO and M. T. TAKEMORI, GE Tech. Inf. Series, no. 82CRD240 (1982).
19. N. J. MILLS and N. WALKER, *J. Mater. Sci.* **15** (1980) 1832.
20. C. BIRKINSHAW, M. BUGGY and J. J. WHITE, *Mater. Chem. Phys.* **14** (1986) 549.
21. BS2782: Part 3: Method 320A to 320F, 1976.
22. ASTM Standard E 647-88, 1988.
23. J. R. WHITE and J. W. TEH, *Polymer* **20** (1979) 764.
24. A. LUSTIGER and R. D. CORNELIUSSEN, *J. Polym. Sci.* B**17** (1979) 269.
25. X. LU and N. BROWN, *J. Mater. Sci.* **21** (1986) 2423.
26. A. LUSTIGER, *ibid.* **22** (1987) 2470.
27. J. JANISZEWSKI, R. W. HERTZBERG and J. A. MASON, *Amer. Soc. Testing Mater. STP* **743** (1981) 125.
28. L. G. LUO and J. D. EMBURY, *Engng Frac. Mech.* **30** (1988) 177.
29. D. S. MATSUMOTO and M. T. TAKEMORI, *J. Mater. Sci.* **20** (1985) 873.

Received 26 February
and accepted 19 March 1991